(article starts on next page)

Fission-fragment yields measured in Coulomb-induced fission of 234,235,236,238U and 237,238Np with the R3B/SOFIA setup

A. Chatillon[1,2,*], G. Boutoux[1], T. Gorbinet[1], L. Grente[1,2], J.-F. Martin[1], E. Pellereau[1], J. Taieb[1,2], H. Alvarez-Pol[3], L. Audouin[4], Y. Ayyad[3], G. Bélier[1,2], J. Benlliure[3], M. Caamaño[3], E. Casarejos[5], D. Cortina-Gil[3], A. Ebran[1,2], F. Farget[6], B. Fernández-Domínguez[3], A. Heinz[7], H. T. Johansson[7], B. Jurado[8], A. Kelić-Heil[9], N. Kurz[9], B. Laurent[1,2], B. Loeher[9], C. Nociforo[9], C. Paradela[3], S. Pietri[9], A. Prochazka[9], D. Ramos[3], J. L. Rodríguez-Sànchez[3], C. Rodriguez[6], D. Rossi[9], H. Simon[9], L. Tassan-Got[4], H. Toernqvist[9], J. Vargas[2], B. Voss[9], and H. Weick[9]

[1]CEA, DAM, DIF, F-91297 Arpajon, France
[2]Université Paris-Saclay, CEA, Laboratoire Matière en Conditions Extrêmes, F-91680 Bruyères-le-Châtel, France
[3]IGFAE, Instituto Galego de Física de Altas Enerxías, Universidade de Santiago de Compostela, E-15782 Santiago de Compostela, Spain
[4]Université Paris-Saclay, CNRS/IN2P3, IJCLab, 91405 Orsay, France
[5]CINTECX, Universidade de Vigo, E-36310 Vigo, Spain
[6]CNRS, GANIL, Bd H. Becquerel, 14076 Caen, France
[7]Chalmers University of Technology, 41296 Gothenburg, Sweden
[8]CNRS, LP2I Bordeaux, F-33175 Gradignan, France
[9]GSI-Helmholtzzentrum fur Schwerionenforschung GmbH, D-64291 Darmstadt, Germany

Abstract. Low energy fission of ^{234,235,236,238}U and ^{237,238}Np radioactive beams, provided by the GSI/FRS facility, has been studied using the R3B/SOFIA setup. The latter allows, on an event-by-event basis, to simultaneously identify, in terms of their mass and atomic numbers, the fissioning nucleus in coincidence with both fission fragments after prompt-neutron emission. This presentation reports on new results on elemental, isobaric and isotopic yields.

1 Introduction

Fission is one of the most dramatic reactions a nucleus can suffer: it leads to extreme deformations, and results in a complete rearrangement of all nucleons. A large variety of observables of the fission process has been probed, both through experimental and theoretical approaches. These observables include the fission cross section, the energy and multiplicity of prompt neutrons and gamma radiations, the yields of the fission fragments, and their kinetic energy. Such observables depend on the isotope which undergoes fission, and the excitation energy at which fission occurs. The R3B/SOFIA (Reactions with Relativistic Radioactive Beams / Studies On FIssion with Aladin) experiment at the GSI/FRS facility focuses on fission yields, which are of high interest, both for application purposes, and for a theoretical description of reactions and the connection to nuclear structure.

In the field of nuclear technology, fission yields are mostly important in nuclear power plants. With increasing use of the fissile fuel, the inventory of fission fragments (and subsequent decay products) becomes more important in the reactor core. Under normal running conditions, some fragments show a very high neutron-absorption cross section: they are thus considered as poisons, and reduce

reactivity. Other fragments emit delayed neutrons, which are essential for the control of the fission rate. In abnormal conditions, the fission chain reaction is stopped, as well as all prompt-energy release. However, the delayed decay of the fission fragments is responsible for the residual power of the core, which amounts to approximately 6% of the nominal value, and decreases steadily with time. An accurate estimate of this decay heat is paramount for the design of cooling systems for the reactor, to cope with this residual energy and to avoid a meltdown of the core. Such an estimate relies on precise and accurate knowledge of yields, half lives and decay energies of the fission fragments.

Fission-fragment yields also probe the influence of nuclear structure of nuclei at extreme deformation on fission, all the more when the yields are correlated with the total neutron multiplicity (ν_{tot}) or the total kinetic energy (TKE). Microscopically the fission process can be described as the evolution of the compound nucleus along the valleys of the potential energy surface (PES), calculated from the binding energy of the system in a given deformation subspace. An interpretation of the fission observables [1] states that each valley results in a different fission mode, each characterized by its own barrier and scission configuration and governed by the shell structure of the nascent fission fragments. In the near-stable actinide re-

---

*e-mail: audrey.chatillon@cea.fr

gion, the focus of this article, a competition between three main fission modes has been proposed. The standard I (ST1) asymmetric mode is governed by the doubly-magic shell closure around ^{132}Sn, leading to an almost spherical heavy fragment and therefore a compact scission configuration. The standard II (ST2) asymmetric mode is characterized by a heavy fragment stabilized around $Z = 54$ [2], which has been related to a proton shell in the octupole-deformed fragments [3]. Finally the super-long (SL) symmetric mode leads to two, on average, mass-symmetric fission fragments, which are both highly deformed. This mode prevails at higher excitation energies, as the microscopic shell structure is progressively dampened.

We present experimental results on the fission yields for ^{234,235,236,238}U and ^{237,238}Np. Fission of these isotopes was induced by Coulomb excitation, with a mean excitation energy for the (γ,f) reaction around 14 MeV [4, 5]. Therefore, as an example, the ^{236}U(γ,f) reaction can be considered as a surrogate reaction for 8 MeV-neutron-induced fission of ^{235}U.

On an event-by-event basis, radioactive beams and fission fragments are identified in terms of their nuclear charge and mass in coincidence. Thus, it beacomes possible to extract fission yields and total prompt-neutron multiplicity. The set-up and the analysis are discussed in detail in Refs. [4–6] and are not described in this article. Only results obtained for elemental, isobaric, isotopic yields are presented in Secs. 2, 3 and 3, respectively.

2 Elemental yields

The elemental yields with their associated uncertainties, measured for ^{234,235,236,238}U(γ,f), are represented in Fig. 1. Thanks to the very high efficiency, the full acceptance of the setup and the good Z-resolution, the uncertainties are dominated by the statistics. For the most populated reaction, ^{236}U(γ,f), the yields are thus obtained with an unprecedented accuracy, below 1% for asymmetric fission, and below 2% for symmetric splits.
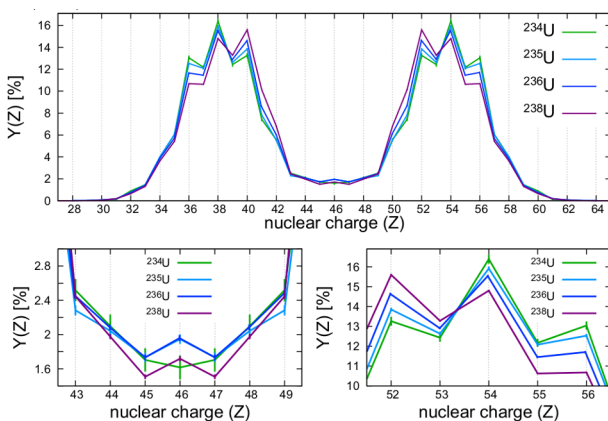

Figure 1. Experimental elemental yields, with their uncertainties, measured for ^{234,235,236,238}U(γ,f) with the R^{3}B/SOFIA setup. Details of the data are exhibited in the lower panels for the specific symmetric (left) and asymmetric (right) fission ranges.

Along the uranium isotopic chain, the distribution of the fission fragments measured within this work, at a similar excitation energy, is rather stable for symmetric scission, but the maximum for asymmetric scission changes from $Z_\mathrm{H} = 52$ in ^{238}U(γ,f) to $Z_\mathrm{H} = 54$ in the lighter isotopes. This originates from a decrease of the influence of the ST1 fission mode when the N/Z ratio of the compound nucleus moves away from that of ^{132}Sn.

Figure 2 shows the comparison of the elemental yields between Coulomb-induced fission of ^{234}U and thermal-neutron induced fission of ^{233}U [7] in the upper panel and Coulomb-induced fission of ^{236}U and thermal-neutron induced fission of ^{235}U [8] in the lower panel. Such a comparison demonstrates the effect of the increased excitation energy of the fissioning nucleus, since Coulomb-induced fission populates the fissioning nucleus with an excitation energy, which is about 8 MeV higher than for thermal-neutron induced fission. Consequently, the SL symmetric mode is more likely to be populated in the data presented here, and the even-odd staggering, characterized by the elemental yields enhancement of the even-Z fission fragments, appears to be considerably reduced.

Odd-Z ^{237,238}Np isotopes were also populated, but with fewer statistics. The elemental yields for ^{237,238}Np(γ,f) are shown in Fig. 3. They are obtained for the most populated elements in asymmetric fission with uncertainties below 5%, and for symmetric fission with uncertainties below 15%. Figure 3 also shows that the most-populated fission-fragment pair is not identical for the two fissioning systems. Whereas the elemental yields are enhanced for the $(Z_\mathrm{L} = 39, Z_\mathrm{H} = 54)$ pair of fission-fragments, with an even-Z_H fission fragment for ^{237}Np(γ,f), it is the
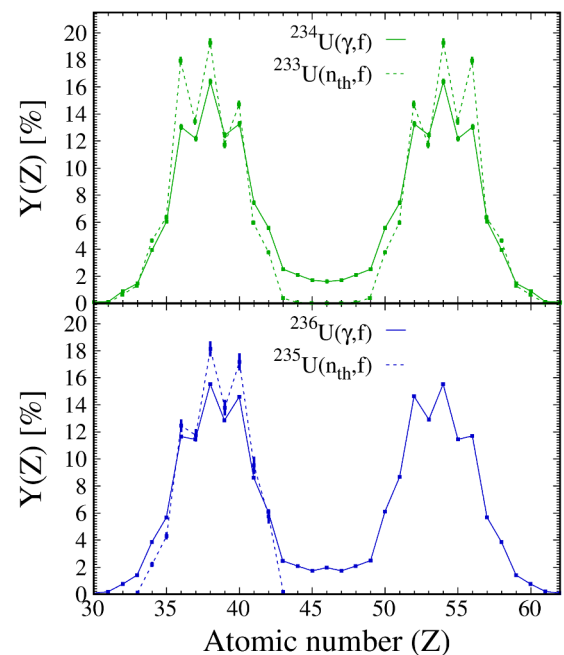

Figure 2. For the fissioning nuclei ^{234,236}U, results are also compared to thermal-neutron-induced fission of ^{233,235}U (dashed lines) from [7, 8], respectively.
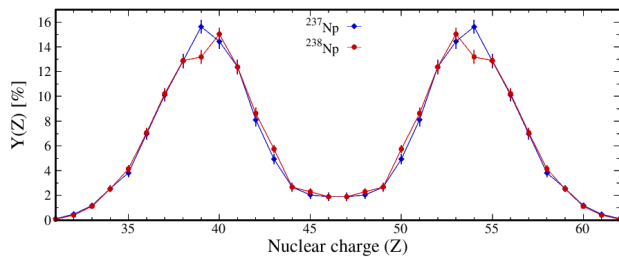
Figure 3. Experimental elemental yields, with their uncertainties, measured for ^{237,238}Np(γ,f) with the R^{3}B/SOFIA setup.

($Z_L = 40, Z_H = 53$) pair characterized by an even-Z_L which is enhanced for the fission of ^{238}Np.

3 Isobaric yields

The isobaric yields measured for ^{234,235,236,238}U(γ,f) and ^{237,238}Np(γ,f) are presented in Figs. 4 and 5, respectively. The peak of the heavier fragments remains approximately centered at the same position for all uranium and neptunium isotopes, while the peak of the lighter fragments moves accordingly to compensate for the variation in the total number of neutrons of the fissioning systems.
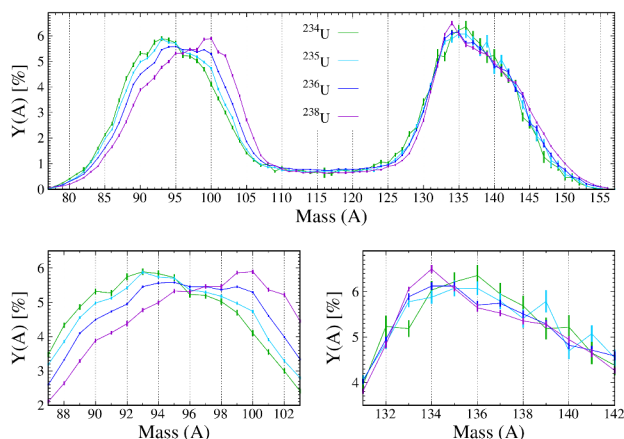

Figure 4. Experimental isobaric yields, with their uncertainties, measured for ^{234,235,236,238}U(γ,f) with the R^{3}B/SOFIA setup. Details of the data are exhibited in the lower panels for the specific symmetric (left) and asymmetric (right) fission ranges.
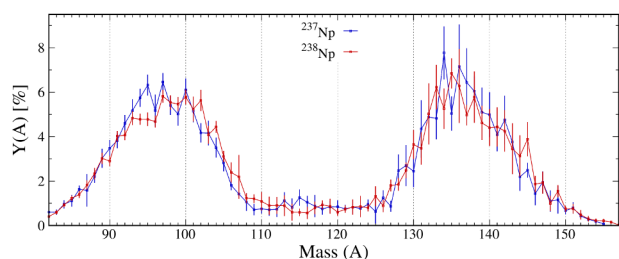

Figure 5. Experimental isobaric yields, with their uncertainties, measured for ^{237,238}Np(γ,f) with the R^{3}B/SOFIA setup.

Figure 6, as for the elemental yields, also presents a comparison of the isobaric yields measured in ^{234,236}U(γ,f)

and ^{233,235}U(n$_{th}$,f), therefore for the same fissioning nuclei ^{234,236}U, but at two different excitation energies. Thermal neutron-induced fission of ^{233}U [7, 9] and ^{235}U [8] show a more asymmetric behavior; the symmetric valley is depleted. In Coulomb-induced fission data, given that the excitation energy is around 7 to 8 MeV higher, the SL symmetric mode populates the range $105 \leq A \leq 130$. Nevertheless, a fine structure observed for the light fragment group, is very similar at both excitation energies. It indicates that the underlying effects responsible for the enhancement of the yields at $A = 90$ and $A = 92 - 95$ are preserved over the large excitation energy range.
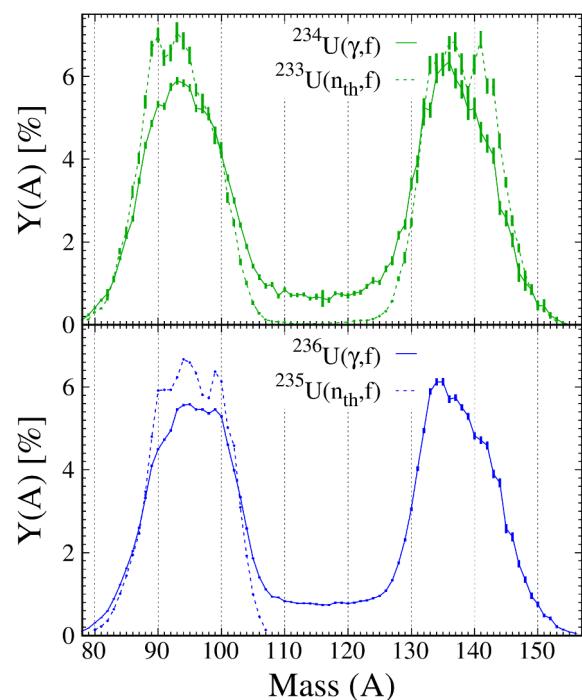

Figure 6. For the fissioning nuclei ^{234,236}U, results are also compared to thermal-neutron-induced fission of ^{233,235}U (dashed lines) from [7, 8], respectively.

Isobaric yields should also be compared to the cumulative yields obtained from radiochemical measurements at different neutron beam energies. As already mentioned in the introduction, the ^{236}U(γ,f) reaction is a surrogate reaction for direct kinematics neutron-induced fission of ^{235}U at a beam energy of around 8 MeV. Therefore the R^{3}B/SOFIA data can be a powerful tool to discriminate between the different existing sets of direct-kinematics data. This is nicely illustrated in the left and central panels of Fig. 7, for the cumulative yields of ^{140}Ba and ^{99}Mo, respectively. Moreover, the right part of Fig. 7 illustrates that our data can also confirm, or not, the values of the different cumulative yields, if the latter are measured during an experiment performed with a neutron beam energy close enough to 8 MeV.
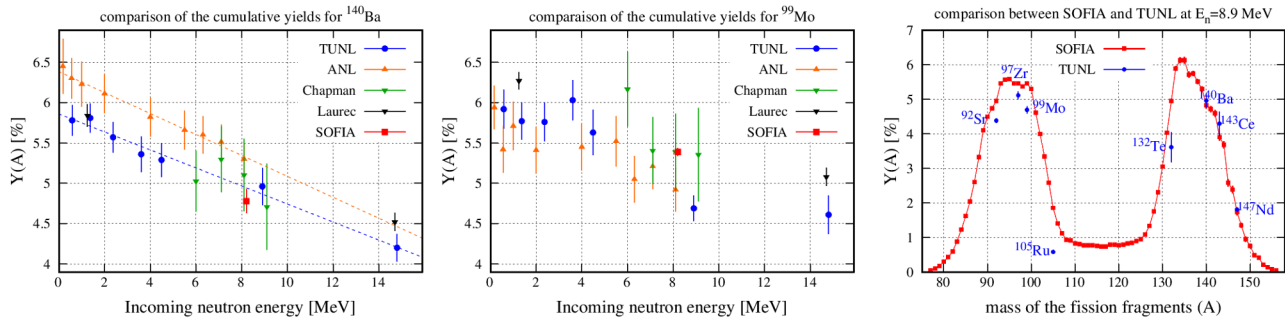
Figure 7. Cumulative yields for ^{140}Ba and ^{99}Mo measured by different sets of data, as function of the neutron beam energy are compared to the R^{3}B/SOFIA isobaric yields for these two specific fragments, in the left and central panels, respectively. In the right panel, all cumulative yields measured at TUNL, applying a radiochemical analysis on ^{235}U(n,f) data with a neutron beam at 8.9 MeV, are compared to the full set of isobaric yields from R^{3}B/SOFIA.

4 Isotopic yields

Only isotopic fission yields obtained for ^{236}U(γ,f) are presented in Fig. 8. The data cover the whole fission fragment charge range from $Z = 30$ to $Z = 60$. Error bars in the figure indicate statistical uncertainties, illustrating the level of accuracy obtained with the R^{3}B/SOFIA setup. For the light fission fragment group, uncertainties are mostly below 1.5%. For the heavy fission fragment group and at symmetry, uncertainties are below 3.5% for the most probable isotopes. Isotopic yields measured for ^{234,235,238}U(γ,f) are detailed in Ref. [5].
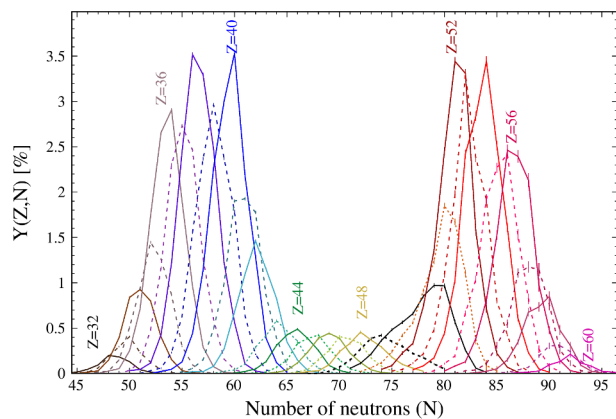

Figure 8. Experimental isotopic yields, with their uncertainties, measured for ^{236}U(γ,f) with the R^{3}B/SOFIA setup. Isotopic yields for $Z = 49$ and $Z = 50$ are represented in black dashed and full lines, respectively.

Finally, it appears that for all elements, the isotopic distribution follows a Gaussian-like distribution, covering eight to twelve neutron numbers. Elements $Z_H = 49$ (in-

dium) and $Z_H = 50$ (tin) show a quite different behavior, with an asymmetric shape. Indium is centered at $N = 74$, and shows a tail which extends up to $N = 80$. In contrast, tin isotopes are centered around $N = 79$, with a tail which extends down to $N = 71$. Therefore, a shift of just one Z unit causes a shift in neutron number of five units.

5 Conclusions

Elemental, isobaric and isotopic yields have been measured for Coulomb-induced fission of the nuclides ^{234,235,236,238}U and ^{237,238}Np. The full fission-fragment range was investigated, using the R^{3}B/SOFIA setup at the GSI/FRS facility. Results are obtained with an unprecedented accuracy for the ^{235,236}U compound nuclei, thanks to an accumulated statistics of more than 10^6 Coulomb-induced fission events.

For the first time, isotopic yields were measured for the compound nuclei ^{237,238}Np. In Ref. [2], it was observed that the Z-value of the heavy fragments provides an enhanced stability. With the R^{3}B/SOFIA experiment, this conclusion has been extended to the ^{237,238}Np fissioning nuclei.

References

[1] U. Brosa, Phys. Rev. C **38**, 1944 (1988).
[2] K.-H. Schmidt *et al.*, Nucl. Phys. A **665**, 221 (2000).
[3] G. Scamps and C. Simenel, Nature **564**, 382 (2018).
[4] E. Pellereau *et al.*, Phys. Rev. C **95**, 054603 (2017).
[5] J.-F. Martin *et al.* Phys. Rev. C **104**, 044602 (2021).
[6] A. Chatillon *et al.*, Phys. Rev. C **99**, 054628 (2019).
[7] U. Quade *et al.*, Nucl. Phys. A **487**, 1 (1988).
[8] W. Lang *et al.*, Nucl. Phys. A **345**, 34 (1980).
[9] F. Martin *et al.*, Nucl. Data Sheets **119**, 328 (2014).